Chemical Papers (2023) 77:2525–2538
https://doi.org/10.1007/s11696-022-02643-w

ORIGINAL PAPER

Selective separation and purification of cerium (III) from concentrate liquor associated with monazite processing by cationic exchange resin as adsorbent

Ahmed M. Shahr El-Din[1] · Hoda E. Rizk[2] · Emad H. Borai[1] · El Sayed M. El Afifi[1]

Received: 10 October 2022 / Accepted: 21 December 2022 / Published online: 3 January 2023

Abstract

The present study is directed to find the optimal conditions required for efficient separation and purification of Ce^{3+} as an analog for lanthanides from Fe^{3+}, Th^{4+}, and Zr^{4+} (interfering ions) using Amberlite IR120H (AIR120H) resin as a strongly cationic exchange adsorbent. The main factors affecting the separation processes had been investigated and optimized. Ce^{3+} (Ln^{3+}) as an admixture with Fe^{3+}, Th^{4+}, and Zr^{4+} was successfully separated by batch and column techniques. The sorption efficiency (*S*, %) from different acidic media was in this order: $HCl > HNO_3 > H_2SO_4$. In a quaternary mixture with Fe^{3+} and Th^{4+}, the maximum separation factor between Ce^{3+} and Zr^{4+} was ~ 13 after 90 min of equilibration, and the sorption capacity of AIR120H resin for Ce^{3+} was 8.2 mg/g. The rate of adsorption was found to follow a pseudo-second-order kinetic model. Separation of the absorbed ions was achieved by desorption processes. Firstly, 98 ± 2% of loaded Ce^{3+} is fully desorbed by 1 M sodium acetate solution without interfering ions. Moreover, ~ 95% of Zr^{4+} is desorbed by 1 M citric acid solution. Finally, 85% of loaded Fe^{3+} and Th^{4+} ions are desorbed with 8 M HCl solution. The batch technique was applied to separate and purify Ln^{3+}-concentrate in chloride liquor ($LnCl_3$), coming from the caustic digestion of Egyptian high-grade monazite. However, the enhanced radioactivity in $LnCl_3$ due to radium -isotopes ($^{228}Ra^{2+}$, $^{226}Ra^{2+}$, $^{224}Ra^{2+}$, $^{223}Ra^{2+}$) and radio-lead ($^{210}Pb^{2+}$) is initially reduced by a factor of 92% (i.e., safe limit) by pH-adjustment. As result, it can be recommended that the sorption process by AIR120H resin is efficient and promising for exploring pure lanthanides from its minerals.

Keywords Lanthanides · Extraction chromatography · Separation · High-grade monazite

Introduction

The degree of purity of lanthanides (Ln^{3+}, 4*f*-elements) plays a significant role in many areas of contemporary techniques. Lanthanides have many scientific applications such as catalysts, synthetic products and a variety of applications in nuclear energy (Du and Graedel 2011; Tian et al. 2012; Metwally and Rizk 2014). Therefore, the production of lanthanides with high purity is very important for such applications. Variable minerals are considered the main sources of lanthanides such as monazite (light Ln-PO_4) (Borai et al. 2017a, b) bastnaesite (Ln-FCO_3) and xenotime (heavy Ln-PO_4) (Rosenblum and Fleischer 1995). Separation of lanthanides from these minerals is usually after concentration, leaching and filtration. The problem is the selective as well as quantitative separation of lanthanides in the presence of impurities from the post-filtration solution. The separation of lanthanides from the most abundant rare earth mineral, i.e., monazite ore is usually associated with impurities such as U(IV), Th(IV), Fe(III), and Zr(IV) (Hamed et al. 2016). The effective separation and purification of lanthanides from these impurities is thus an interesting step. Most of the studies under this aim usually utilize the traditional precipitation method (Abreu and Morais 2010; Borai et al. 2018; Kumari et al. 2018; Rodliyah et al. 2015). The disadvantages of the precipitation method are that more time is spent in digest, filtering, or washing and disposal the precipitates, limited recovery of rare earths, highly dependent on pH that Ln^{3+} can co-precipitate with Th and U with any error in the

✉ Hoda E. Rizk
ahmhoda@gmail.com

[1] Analytical Chemistry and Control Department, Hot Laboratories and Waste Management Center, Egyptian Atomic Energy Authority, Cairo 13759, Egypt

[2] Nuclear Fuel Technology Department, Hot Laboratories and Waste Management Center, Egyptian Atomic Energy Authority, Cairo 13759, Egypt

detection of the pH value, and pollution from the storage of radioactive precipitate (Ang et al. 2018; Wang et al. 2013). On the other hand, the ion exchange technique is the most suitable separation technique due to its non-complication as associated with solvent extraction due to less use of organic solvent and less waste accumulation (Mayyas et al. 2014; Rizk et al. 2022a; Rodríguez et al. 2016; Shu et al. 2018; Zhang et al. 2004) and overcomes the traditional precipitation method problems, as well as the ability of ion exchangers and chelating resins to extract Ln^{3+} from dilute solution (Esma et al. 2014). Monazite is the main source of lanthanides and thorium in the world. In Egypt, monazite contains on average 50% lanthanide as Ln_2O_3. The concentration of cerium in Ln_2O_3 cake was ~ 45% (Ali et al. 1996). So, recovery and separation of lanthanides from monazite-cake require quantitative removal of the interfering metal ions as Zr^{4+}, Th^{4+}or Fe^{3+}. Therefore, the efficiency of Amberlite IR120H resin as a cation exchanger for separation and purification of Ce^{3+} as analog for lanthanides from Zr^{4+}, Th^{4+}, and Fe^{3+}, commonly exist in monazite, with high purity and yield were studied to determine the optimum conditions for separation of Ce^{3+} from these undesirable ions using batch and column technique. Further, the obtained optimum conditions will be applied to separate and purify Ln(III)-concentrate from the caustic digestion of Egyptian high-grade monazite.

Experimental

Materials and reagents

All reagents used were of high analytical grade and used without further purification. Herein, the solid phase extraction is done by strongly cationic exchanger resin, Amberlite IR120H resin as AIR120H. The chemical structure of the AIR120H resin is represented in Fig. 1, while its main physicochemical characteristics are listed in Table 1. The AIR120H resin is provided from the BDH Chemical Co. (England), while $FeCl_3$, $ZrOCl_2$, $Th(NO_3)_4$ and $CeCl_3{\cdot}7H_2O$ were obtained from Sigma-Aldrich. High-grade monazite concentrate (> 90%) was supplied by the Egyptian nuclear materials authority.

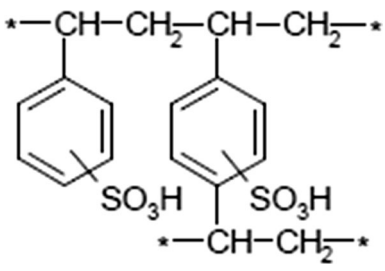

Fig. 1 The chemical structure of AIR120H resin (Attallah et al. 2020)

Table 1 Main characteristics of the Amberlite IR120 resins (AIR120H) (Rizk et al. 2022b)

Properties	Amberlite IR120H
Function group	Sulfonic,–SO_3H
Matrix	Poly styrene
Structure	Macroporous
pH range	0.0–14
Bead size	0.3–1.0 mL
Capacity	5.4 mg eq/L

Sorption experiments

Experiments of the solid phase extraction by AIR120H resin have been done to evaluate the feasibility of separation of Ce^{3+} as analog for lanthanides (Ln^{3+}) from the undesired metal ions, e.g., Fe^{3+}, Th^{4+} and, Zr^{4+}. The sorption experiments were performed assuming 100 ppm for each metal ion in all the studied solution systems (single or quaternary). In batch investigations, 5 mL of the prepared metal ion solution is mixed with 0.05 g of AIR120H resin, i.e., *V*/*m* is 0.1 L/g at room temperature. The parameters of sorption efficiency (*S*, %), sorption capacity (mg/g), distribution coefficient (K_d, mL/g) and separation factor (SF) were defined by the next empirical formulas (El Afifi et al. 2016; Dakroury et al. 2020):

$$\text{Sorption efficiency } (S,\%) = \frac{C_o - C_e}{C_o} \times 100 \quad (1)$$

$$\text{Sorption capacity, mg/g} = \left(C_o - C_e\right) \times \frac{V}{m} \quad (2)$$

$$\text{Distribution coefficient } \left(K_d\right), \frac{\text{mL}}{\text{g}} = \frac{C_o - C_e}{C_e} \times \frac{V}{m} \quad (3)$$

$$\text{Separation factor (SF)} = \frac{K_{d(A)}}{K_{d(B)}} \quad (4)$$

where C_o and C_e are the initial and final concentrations of metal ions, respectively, while *V* and *m* represent the solution volume (L) and adsorbent mass (g). Moreover, the extraction chromatography had also been carried out using a glass column with 8 mm (internal diameter, ϕ) and 100 mm (length *l*) with constant flow rate of 0.5 mL/min. Also, several solutions were examined for the desorption process of the loaded metal ions onto the resin. All experiments were

carried out as duplicate determinations with standard uncertainty below 5%.

Instrumentation

The initial and final concentrations of the studied metal ions were measured by a Cintra UV–visible spectrophotometer; model Cintra 2.2 (model Cintra 2.2, Australia). However, concentrations of Ce^{3+} and Zr^{4+} were measured as colored complexes by Arsenazo-III method at wave lengths of λ_{max} 650 ± 2 and 665 ± 2 nm, respectively (Marczenko 1976). The concentration of Th^{4+} was measured by the Thoron-I method as colored complex at 540 ± 2 nm, while Fe^{3+} was measured by thiocyanate method at 495 ± 2 nm (Marczenko 1976). On the other hand, the radiometric measurements were done using multichannel NaI(Tl) scintillation detector and high purity germanium detector, Canberra Industries Inc. (USA) (Wang et al. 2015). The metal concentrations of $LnCl_3$ after deactivation were measured using ICPS-7500 (Shimadzu Sequential Plasma Spectrometer, Japan). The possible speciation diagrams of the metal ions have been done in HCl solution using HYDRA-MEDUSA-32 software (version 2009, Sweden) (Dakroury et al. 2020). The hydrogen ion concentration of the working solutions was adjusted using 0.1 M HCl or NaOH by pH-meter with accuracy of ± 0.1.

Results and discussion

Exploration of monazite mineral to obtain lanthanides as a strategic product face two opportunities, these are how to minimize the major undesired metallic impurities (e.g., Fe, Zr, Th) associated with lanthanides (Ln^{3+}) in the chloride liquor and the enhanced natural radioactivity due to presence radium-isotopes (^{228}Ra, ^{226}Ra, ^{223}Ra) and radio-lead ($^{210}Pb^{2+}$). Therefore, the required conditions for the efficient separation of lanthanides were investigated assuming simulated solutions containing Ce^{3+} as analog for lanthanides and Fe^{3+}, Th^{4+} and Zr^{4+} as interfering metal ions commonly exist in monazite or its corresponded Ln(III)-liquors. Hence, the optimized conditions will be applied for the purification of real lanthanide liquor from the enhanced natural radioactivity level and the undesired metallic impurities.

Factors affecting the separation conditions

Some factors had been investigated to find sorption behavior of Ce^{3+} ions and the interfering metal ions, e.g., Fe^{3+}, Th^{4+} and Zr^{4+} by AIR120H resin as strongly cationic adsorbent. Thus, different parameters included acid solution type, acid concentration, and equilibration periods were studied to find the optimum conditions required for the efficient separation of Ce^{3+} from the interfering metal ions (Fe^{3+}, Th^{4+}, Zr^{4+}) of our interest, as listed below.

Acid solution type

For this purpose, the sorption behavior of 5 ml from100 ppm Ce^{3+} (i.e., Ln^{3+}) as well as Fe, Th and Zr was investigated individually in different acidic solutions of 0.1 M HCl, HNO_3 and H_2SO_4 solutions, using 0.05 g of AIR120H resin with contact time, 2 h and room temperature. The results are given in Fig. 2. It is observed that the sorption efficiency (*S*, %) of the metal ions was significantly varied with the investigated acid solution type in accordance as $HCl > HNO_3 > H_2SO_4$. The lower sorption efficiency from H_2SO_4 media may be related to the dissociation of sulfuric acid giving two hydrogen atoms that compete with the cation on the active site of the resin. On the other hand, the removal efficiency from hydrochloric acid is more favorable than nitric acid may be due to the higher electronegativity of NO_3^- than for Cl^- ion and may be masking for the cations. The increase in the sorption efficiency of Amberlite IR120 resin from HCl more than HNO_3 has been mentioned also in our previous work (Rizk et al. 2022b).

It is found that the *S*, % of metal ions in 0.1 M HCl solution was high and approximately similar to around 93 ± 2% for Ce^{3+}, Fe^{3+} and Th^{4+}; while was low for Zr^{4+}, (i.e., 40 ± 2%). In 0.1 M nitric acid solutions, the S, % is decreased to 80 ± 2, 55 ± 3, 74 ± 2 and 36 ± 3% for Ce^{3+}, Fe^{3+}, Th^{4+} and Zr^{4+}, respectively. The larger decrease in *S*, % is found in sulfuric acid solution. The values of *S*, % are decreased to 13 ± 1, 7 ± 1, 25 ± 2 and 8 ± 1.1% for Ce^{3+}, Fe^{3+}, Th^{4+} and Zr^{4+}, respectively (Fig. 2). As a result, 0.1 M hydrochloric acid solutions are highly efficient compared with nitric or sulfuric acid solutions, thus, it is chosen as a

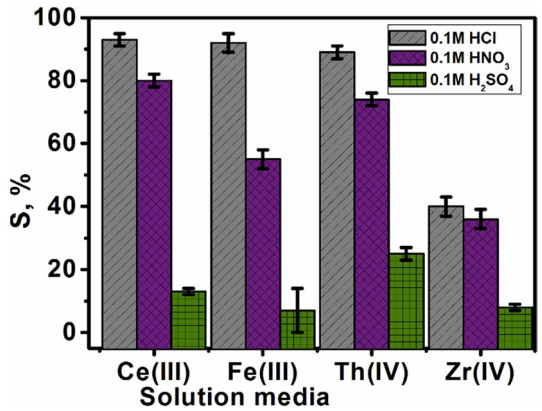

Fig. 2 Influence of 0.1 M of different solution media on the sorption of 100 ppm of Ce^{3+}, Fe^{3+}, $Th^{4+}$and Zr^{4+} ions by 0.05 g of AIR120H resin as adsorbent at *V*/*m* ratio, 0.1 g/L, contact time 2 h and 25 ± 0.3 °C

suitable medium to investigate the further parameters affecting on the sorption behavior of the studied metal ions.

Concentration of HCl solutions

The influence of HCl solutions on the sorption behavior of all the studied metal ions (100 ppm) and contact time, 2 h, is investigated within the concentration range 0.001–5 M. The sorption process is done individually by the used AIR120H resin. The results are illustrated in Fig. 3.

It is observed that the *S*, % of all metal ions is high in diluted solutions (0.001–0.1 M HCl), then, decreased gradually to1 M, followed by a rapid decrease to 5 M HCl. The sorption behavior of Ce, Fe and Th is almost similar compared to Zr. The *S*, % of Ce, Fe and, Th was in the average 95 ± 2% within 0.001–0.1 M HCl, while it was about 40 ± 3% for Zr. Over 0.1 M HCl leads to a significant decrease in the *S*, %. It is found that the *S*, % of Ce, Fe, Th and Zr at 1 M HCl solution is decreased to 72 ± 3, 65 ± 2, 58 ± 2 and 18 ± 2%, respectively. On the other hand, the *S*, % of all metal ions was nil at 5 M HCl, Fig. 3. The decrease in the *S*, % may be due to a larger competition between the positively charged species of the studied metals with protons as result of the high acid concentration to be chelated with resin sulfonic moieties (El Afifi et al. 2016; Rizk and El-Hefny 2020). Thus, 0.01 M HCl (pH 2) is chosen as suitable and efficient solution for sorption of the metal ions in the next investigations. As reported by Hamed et al., this value of pH (pH 2) was suitable for selective separation of Fe^{3+} from U^{4+}, Th^{4+}, and Ce^{3+} using nanocomposite of polyaniline functionalized Tafa (Hamed et al. 2019). To know the sorption mechanism between the studied metal ions with active sites of the used AIR120H resin, speciation diagrams of Ce^{3+}, Fe^{3+}, Th^{4+}, and Zr^{4+} have been constructed in Fig. 4a–d. It is observed that all metal ions were adsorbed onto the resin as a result of the ion exchange process between the resin sulfonic moieties, i.e., $–SO_3H$, and the positively charged species of the metal ions. Regarding Fig. 3, the high *S*, % was obtained at 0.001–0.1 M HCl (i.e., pH 1–3); this means that the metal ions created a positively charged species with the resin sulfonic moieties, i.e., $–SO_3H$. Thus, Ce ions are adsorbed by ion exchange interaction as Ce^{3+}, $CeCl^{2+}$ and/or $CeCl_2^{+}$ (Fig. 4a) with the resin moieties. This concept can be also said for the other metal ions, i.e., Fe^{3+} or Th^{4+}, with AIR120H resin moieties with pH's < 3, however, Fe^{3+} ions exist as species of Fe^{3+}, $FeOH^{2+}$, $FeCl^{2+}$ and/or $FeCl_2^{+}$ (Fig. 4b); Th ions present as different species as Th^{4+}, $ThCl^{3+}$, $ThOH^{3+}$, $ThCl_2^{2+}$ or $Th(OH)_2^{2+}$ (Fig. 4c); Zr exists as species of $Zr_4(OH)_8^{8+}$, $Zr_3(OH)_5^{7+}$, Zr^{4+}, $ZrOH^{3+}$, $Zr(OH)_2^{2+}$ or $Zr(OH)_3^{+}$ (Fig. 4d). As seen in Fig. 4d, presence of bigger and bulkier positively charged species of Zr like $Zr_4(OH)_8^{8+}$ and/or $Zr_3(OH)_5^{7+}$, as well as the higher free energy of hydration for Zr, may explain the lower affinity of Amberlite IR-120 toward Zr (Rizk et al. 2022b). It is common knowledge that metals have a stronger tendency to stay in the liquid phase and hydrate more water molecules as their absolute hydration free energy increases (Xu et al. 2021; Wang et al. 2020; Speight 2005). The free energy of hydration for Zr is higher than that for Th, Fe, and Ce (Wang et al. 2020; Mokhtari and Keshtkar 2016; Talebi et al. 2017). Therefore, Zr is more likely than Th, Fe, and Ce to remain in the liquid phase more than adsorbed in the resin. The possible ion exchange mechanism for sorption of the metal ions with AIR120H resin can be simply represented as

$$\text{For } M^{3+}\left(Ce^{3+}\left(Ln^{3+}\right) \text{ or } Fe^{3+}\right): M^{3+} + 3AIR-SO_3H \leftrightarrow M\left(AIR-SO_3\right)_3 + 3H^{+} \quad (5)$$

$$\text{For } M^{4+}\left(Th^{4+} \text{ or } Zr^{4+}\right): M^{4+} + 4AIR-SO_3H \leftrightarrow M\left(AIR-SO_3\right)_4 + 4H^{+}. \quad (6)$$

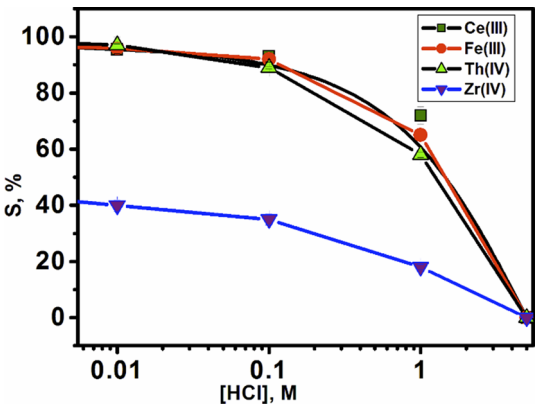

Fig. 3 Influence of HCl concentration (M) on the sorption of 100 ppm of Ce^{3+}, Fe^{3+}, $Th^{4+}$and Zr^{4+} ions by 0.05 g of Amberlite-IR120H resin at V/m ratio, 0.1 g/L, contact time 2 h and 25 ± 0.3 °C

Equilibration periods

It is well known that contact time is one of the predominant factors governing the distribution of the metal ions between two phases. (Satusinprasert et al. 2015). The sorption behavior of Ce^{3+}, i.e., Ln^{3+}, is investigated with Fe^{3+}, Th^{4+} and Zr^{4+} as interfering metal ions in admixture to simulate the presence of lanthanides in monazite matrix or its corresponded lanthanide chloride liquor ($LnCl_3$). The sorption performance of the investigated ions in admixture from 0.01 M HCl solution was conducted at different intervals ranging from 15 to 120 min. and *V*/*m* ratio of 0.1 L/g at 25 ± 1 °C. Figure 5 shows that the *S*, % of all metal ions from admixture is decreased than from single

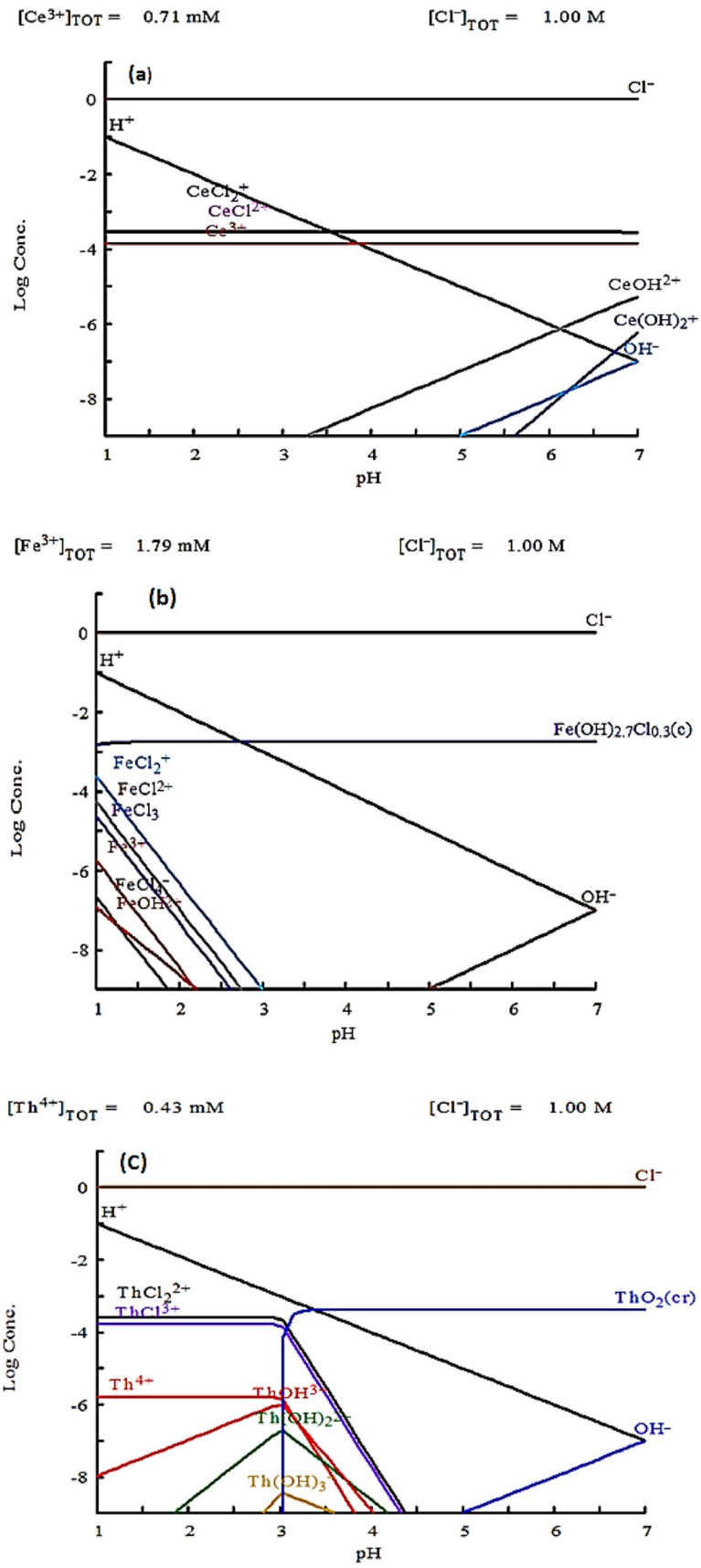

Fig. 4 Speciation diagram of **a** Ce^{3+}, i.e., Ln^{3+}, **b** Fe^{3+}, **c** Th^{4+} and **d** Zr^{4+}

Fig. 4 (continued)

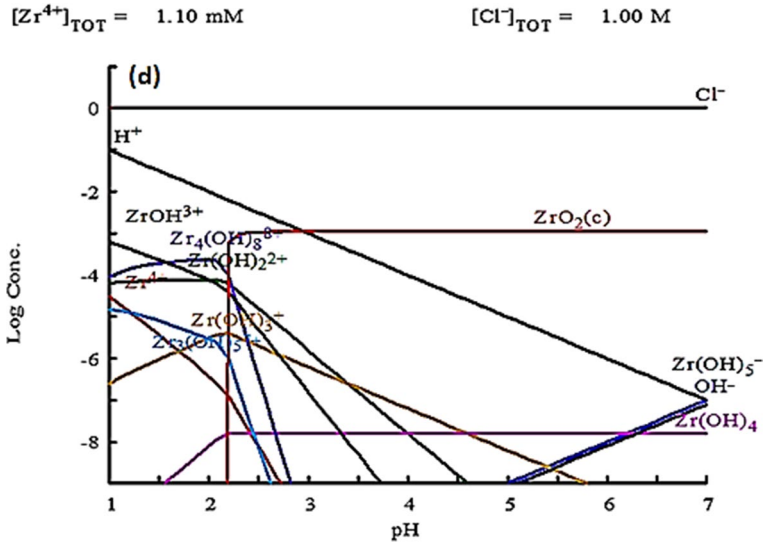

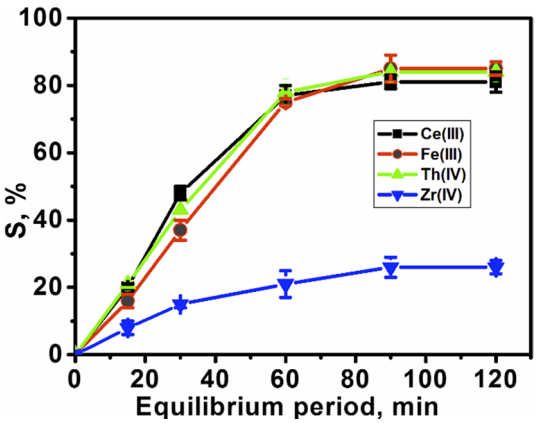

Fig. 5 Influence of equilibration periods on the sorption of 100 ppm of Ce^{3+}, Fe^{3+}, $Th^{4+}$and Zr^{4+} ions in admixture by 0.05 g of AIR120H resin at *V*/*m* ratio, 0.1 g/L, and 25 ± 0.3 °C

Table 2 Influence of equilibration periods on values of K_d (mL/g) and SFs of Ce (~Fe~Th) and Zr between the admixture solution and AIR120H resin

Time, min	q_e, mg/g		K_d, mL/g		$SF^{Ce^{3+}}_{Zr^{4+}}$
	Ce^{3+} ~Fe^{3+} ~Th^{4+}	Zr^{4+}	Ce^{3+}	Zr^{4+}	
0.0	0.0	0.0	0.0	0.0	0.0
15	1.9	0.8	23.5	8.7	2.7
30	4.3	1.5	75.4	17.6	4.3
60	7.7	2.1	334.8	27.0	12.4
90	8.2	2.6	455.6	35.1	12.98
120	8.2	2.6	455.6	35.1	12.98

system (Figs. 2, 3). This result can be attributed to the increase in the total concentration of ions in the solution that have competitive effect on the active sites of sulfonic moieties, i.e., $–SO_3H$, on the surface of the used resin. The main sorption parameters described in Eqs. (2–4) are calculated and given in Table 2. It is observed that the all sorption parameters (*S*, %—sorption capacity, mg/g–K_d, mL/g–SFs) of the studied metal ions are increased through the first 30 min., followed by a slow increase till one hour. Therefore, 90 min. is enough time to attain constant equilibration for the studied metal ions. Hence, the maximum *S*, % at 90 min was ~ 82 ± 2% for Ce^{3+} ~ Fe^{3+} ~ Th^{4+} and was about 26 ± 2% for Zr^{4+}. The initial fast increase in the sorption parameters may be due to the existence of numerous vacant active sites on the surface of AIR120H resin at the initial stage, which was occupied by the metal ions with the increase in the contact time (Shahr El-Din et al. 2019).

The values of the SFs between Ce^{3+} (i.e., Ln^{3+}) and Zr^{4+} are rapidly increased till one hour, then, the high SF values are attained within equilibration periods of 1–2 h. Thus, the maximum SF between Ce^{3+} and Zr^{4+} in quaternary admixture with Fe^{3+} and Th^{4+} was 12.98 at an equilibration period of 90 min, Table 2. Further, the results at equilibrium are compared with those reported elsewhere in the literature. Regarding the sorption capacity obtained herein, it is found that the sorption capacity of Ce^{3+} found by AIR120H resin (q_e, 8.2 mg/g) was larger than that reported by Jian et al., (q_e, 2.5 mg/g) (Jain et al. 2001), close to that found by Gok et al. (2007) (q_e, 8.3 mg/g) and below that reported by Bhatt et al. (2014) (q_e, 86.4 mg/g) for sorption of Ce^{3+} using different sorbents. The variations between the obtained results herein and those reported can be due to differences in their experimental conditions. In the case of separation factor, the values of separation factor of Ce^{3+} are still very limited by solid phase extraction (SPE). Herein, the SF value of Ce^{3+}/Zr^{4+} is low relative to those reported by Eusebius et al. (1977) to separate Ce^{3+} from Ce^{4+} and UO_2^{2+}

Table 3 Comparison for separation factors of Ce^{3+} relative to various metals

Ce^{3+}/M	System mode (SPE/SE)[b]	SFs	References
Zr^{4+}	SPE: AIR120H	12.98	The present work
Ce^{4+}	SPE: Dowex 50W-X8	195	Eusebius et al. (1977)
UO_2^{2+}	SPE: Dowex 50 W-X8	258	Eusebius et al. (1977)
La^{3+}	SE: BLPhen[b]/0.9 M HNO_3	1.7	Healy et al. (2019)
Pr^{3+}	SE: BLPhen/0.9 M HNO_3	8.1	Healy et al. (2019)
Eu^{3+}	SE: ATCO-DCE[c]/LA[d] pH 6–7	2.5	Masuda et al. (1998)

[a]Solid phase extraction (SPE)/solvent extraction (SE)

[b]Bis-lactam-1,10-phhenanthrolin

[c]1,4,10,13-Tetrathia-7,16-diazacyclooctadecane-dichloroethane

[d]Lauric acid

in ammonium acetate solution using Dowex 50 W-X8 resin as cationic adsorbent. On the other hand, the SF for Ce^{3+}/Zr^{4+} is relatively high relative to those obtained by solvent extraction technique as reported by Healy et al. (2019) to separate Ce^{3+} from La^{3+} or Pr^{3+} in 0.9 M HNO_3 solution; or Masuda et al. (1998) to separate Ce^{3+} from Eu^{3+} in aqueous solution (pH 6–7), Table 3.

As can be seen from the previous results, separation of Ce^{3+} was not achieved yet. Therefore, the desorption process for separation of Ce^{3+} from majority Fe^{3+}, Th^{4+}, and minors of Zr^{4+} loaded onto AIR120H resin is investigated below.

Adsorption kinetic study

After studying appropriate contact time for adsorption of Ce^{3+}, Fe^{3+}, Th^{4+}, and Zr^{4+} using AIR120H resin, it is important to establish the sorption kinetic models in order to examine the controlling mechanism of the adsorption process. Therefore, the experimental sorption data were analyzed using the linear form of pseudo-first-order (Lagergren 1898) Eq. (7), pseudo-second-order (Ho and Mckay 1999) Eq. (8).

$$\log\left(q_e - q_t\right) = \log q_e - \frac{K_1}{2.303}t \tag{7}$$

$$\frac{t}{q_t} = \frac{1}{K_2 q_e^2} + \frac{1}{q_e}t \tag{8}$$

In these formula, q_e and q_t are the concentration of the metal ion sorbed at equilibrium and at time t (mg/g) and k_1 (min^{-1}) and k_2 (g/mg min) are the pseudo-first-order and second-order rate constant, respectively. The initial sorption rate, h (mg/g min) at $t \to 0$, is calculated using the second-order rate constant k_2 as follows:

$$h = k_2 q_e^2 \tag{9}$$

Figure 6a, b shows the results of the two kinetic models, and their kinetic parameters are given in Table 4. It was demonstrated that good linear correlation factor (R^2) values were obtained for both the first and second kinetic models, especially for adsorption of Fe^{3+} and Th^{4+}, but that pseudo-second-order achieved closer agreement between theoretical and experimental q_e values for all investigated ions. These findings demonstrate that the pseudo-second-order kinetics for the whole sorption period accurately describes the sorption data. These data imply that the chemisorption process appears to be in control of the overall rate of these metal ions adsorption process (Patawat et al. 2020; Pathania et al. 2017). The exterior liquid film diffusion, surface adsorption, and intra-particle diffusion processes that coexisted during adsorption are also explained by this model (Fan et al. 2017; Patawat et al. 2020).

Desorption investigation

The desorption process is mainly aimed at liberating Ce^{3+}, i.e., Ln^{3+}, separately without interfered metal ions (Fe^{3+}, Th^{4+} and Zr^{4+}) as possible. For this purpose, several solutions including double distilled water (DDW) and 1 M of

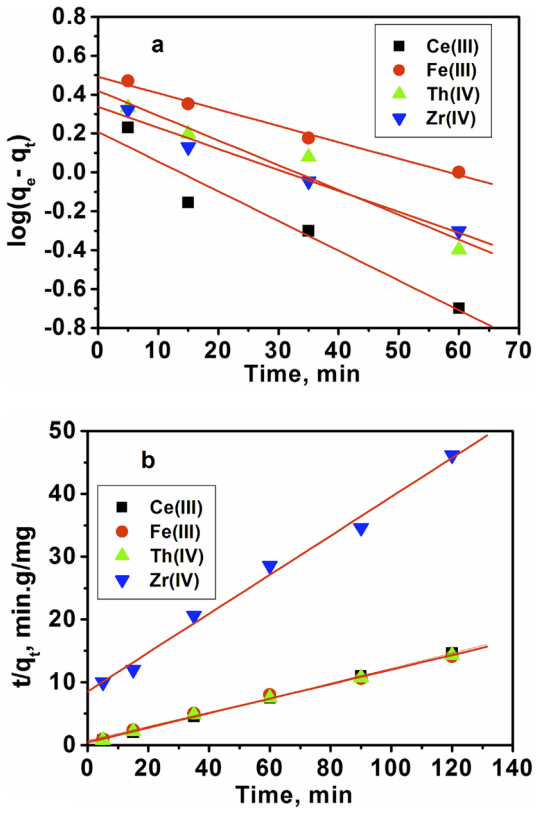

Fig. 6 The pseudo-first-order (**a**) and second-order kinetic (**b**) for adsorption of Ce^{3+}, Fe^{3+}, Th^{4+} and Zr^{4+} ions on AIR120H resin. 25 ± 0.3 °C

Table 4 The calculated parameters of the pseudo-first-order and pseudo-second-order kinetic models of Ce^{3+}, Fe^{3+}, Th^{4+} and Zr^{4+} at 25 ± 1 °C

Ion	Pseudo-first-order parameter			Pseudo-second-order parameter				q_{exp} (mg/g)
	K_1 (min^{-1})	q_{cal} mg/g	R^2	k_2 (g/mg min)	q_{cal} mg/g	h (mg/g min)	R^2	
Ce^{3+}	0.0158	1.2	0.776	0.013	8.8	1	0.998	8.2
Fe^{3+}	0.036	5.27	0.996	0.0045	9.5	0.365	0.99	8.5
Th^{4+}	0.033	7.39	0.998	0.01	9	0.81	0.998	8.4
Zr^{4+}	0.037	4	0.733	0.022	2.9	0.185	0.988	2.6

sodium chloride, citric acid, sodium sulfate, sodium acetate, hydrochloric acid, and ammonium thiocyanate solutions had been examined for desorption of the metal ions loaded onto the AIR120H resin. Firstly; quaternary admixtures of Ce, Fe, Th and Zr (100 ppm for each) were prepared in 0.01 M HCl solution, then, loaded onto the AIR120H resin for equilibration after 90 min assuming *V*/*m* ratio of 0.1 L/g at room temperature. However, the resin-loaded by metal ions is filtered off and submitted for desorption process. Secondly; the loaded resin samples were desorbed by equilibrated with 5 mL of the examined solution for 90 min (*V*/*m*) ratio of 0.1 L/g at room temperature. Then, the desorption efficiency (*D*, %) of certain metal ion from the AIR120H resin is calculated according to (Rizk and El-Hefny 2020):

$$\text{Desorption efficiency}(D,\%) = \frac{C_D}{C_L} \times 100 \quad (10)$$

where C_L and C_D represent concentration of the adsorbed and desorbed metal ions, respectively. The values of *D*, % using several solutions as eluents are given in Table 5.

It is found that desorption of the loaded metal ions was nil by using double distilled water (DDW), HCl, or NH_4SCN solutions. Further, 47 ± 1% and 98 ± 2% of adsorbed Ce^{3+} are desorbed by using 1 M of NaCl and Na_2SO_4 solutions but contaminated with 90% and 95% of Zr^{4+} as an interfered metal ion using both solutions, respectively. Next, 98 ± 2%, i.e., 80.4 ± 1.6 ppm of Ce^{3+} is fully desorbed by 1 M sodium acetate solution, while Fe^{3+}, Th^{4+}, and Zr^{4+} are not desorbed using the mentioned solutions. This means that Ce^{3+} is successfully separated without ions interference. Moreover, ~ 95%, i.e., 24.7 ± 0.8 ppm of Zr^{4+} is desorbed by 1 M citric acid solution, while Ce^{3+}, Fe^{3+} and Th^{4+} are not detected (ND). The subsequent batch desorption had been suggested for successive separation of Ce^{3+} from Fe^{3+}, Th^{4+}, and Zr^{4+} loaded as a quaternary admixture in 0.01 M HCl solution onto AIR120H resin. The desorption processes had been done successively for the loaded AIR120H resin sample under equilibrium conditions using 1 M sodium acetate solution followed by 1 M citric acid, and finally, the used sample washed by 8 M hydrochloric acid solution (used for the flushing of the resin after desorption process) after 90 min of contact time. Figure 7 shows that 98 ± 3% of loaded cerium ions are efficiently separated with purity of 100% in presence of interfering metal ions, e.g., Fe^{3+}, Th^{4+} and Zr^{4+}, simulating lanthanide concentrate solutions associated with monazite mineral processing, using 1 M sodium acetate solution. Finally, 87% of loaded Zr^{4+} ions are desorbed with 1 M citric acid then the remained metal ions (Fe^{3+} and Th^{4+}) are desorbed with about 85%, i.e., (69 ± 2 ppm) of loaded ions when the AIR120H resin is flushed by 8 M hydrochloric acid solution. The influence of sodium acetate concentrations on the desorption and separation of Ce^{3+} from Fe^{3+}, Th^{4+}, and Zr^{4+} loaded on AR120H resin had been also investigated within the concentration range (0.25–1.5 M). The results are given in Fig. 8. It is

Table 5 Sorption and desorption processes of Ce^{3+}, Fe^{3+}, Th^{4+} and Zr^{4+} by AIR120H resin

Process	Metal ions			
	Ce^{3+} (Ln^{3+})	Fe^{3+}	Th^{4+}	Zr^{4+}
A. Loading in 0.01 M HCl, % (ppm)	82	79	82	25
B. Desorption, % (ppm)				
DDW	ND	ND	ND	ND
1 M HCl	ND	ND	ND	ND
1 M NH_4SCN	ND	ND	ND	ND
1 M NaCl	47 ± 3% (38.5 ppm)	ND	ND	90 ± 3% (22.5 ppm)
1 M Na_2SO_4	98 ± 2% (80.36 ppm)	ND	ND	95 ± 2% (23.8 ppm)
1 M CH_3COONa	98 ± 2% (80.4 ± 2 ppm)	ND	ND	ND
1 M Citric acid	ND	ND	ND	90% (22.5 ppm)

DDW: double distilled water, ND: not desorbed

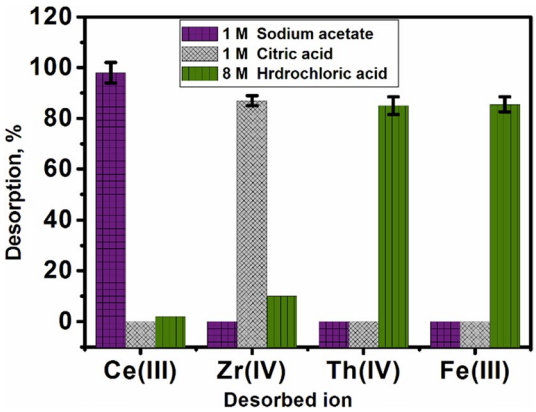

Fig. 7 Sequential desorption process of loaded ions into AIR120H resin using 1 M of sodium acetate, citric acid and 8 M hydrochloric acid. *V*/*m* ratio, 0.1 L/g, 90 min contact time and at 25 ± 1 °C

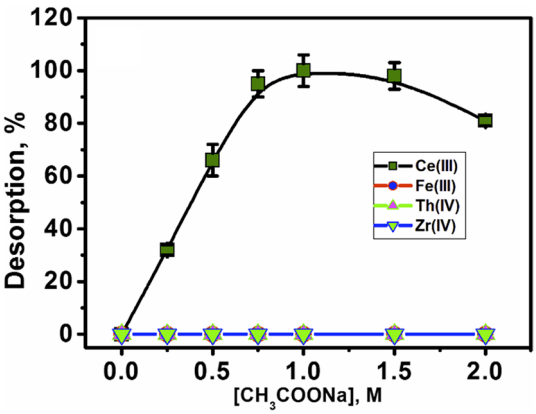

Fig. 8 Influence of sodium acetate concentrations on desorption efficiency of Ce^{3+}, Fe^{3+}, $Th^{4+}$and Zr^{4+} ions loaded into IR120H resin after 90 min of contact time, *V*/*m* ratio of 0.1 L/g, and at 25 ± 1 °C

observed that the *D*, % increases sharply with an increase in the concentration of the eluent till reaches equilibrium. As a results, 1 M of sodium acetate solution is suitable and efficient for desorption of Ce^{3+} ions as a pure solution without interfering with metal ions of Fe^{3+}, Th^{4+} or Zr^{4+}.

Column technique

Assuming the subsequent conditions for sorption and desorption of Ce^{3+} in quaternary admixture with Fe^{3+}, Th^{4+} and Zr^{4+} by batch technique, the solid phase extraction (SPE) is examined by column technique using AIR120H resin as cationic exchange as adsorbent. For this purpose, a pre-cleaned glass column (∅= 8 mm, *L* = 100 mm) is packed with a pre-conditioned AIR120H resin by double distilled water (DDW) for 24 h. The height of the resin in the column was adjusted to 4 ± 0.1 cm, and a steady flow rate of 0.5 mL/min of DDW, then 0.01 M HCl solution (2 × 15 mL) was used to condition the column. The column is kept wet before use. An admixture containing Ce^{3+} (i.e., Ln^{3+}) with Fe^{3+}, Th^{4+} and Zr^{4+} (100 ppm for each) is prepared in 0.01 M HCl solution. An accurate 5 mL of the admixture solution is loaded onto the pre-conditioned column resin bed (AIR120H). For desorption process, the column bed is rinsed by 3 × 5 mL of sodium acetate solution (1 M) then citric acid (1 M) and followed by 8 M HCl solution (used for the flushing process of the column resin after the elution process), with a constant flow rate of 0.5 mL/min. Hence, the effluents associated with the loading and elution processes of the column resin were measured to evaluate the amount of metals loaded onto the column resin or eluted from the column itself. The obtained results for loading and elution through the suggested column resin technique are demonstrated in Fig. 9.

It is found that the loading efficiency (*L*, %) of the metal ions onto the column resin was 69 ± 4, 65 ± 3, 67 ± 4 and 21 ± 2% for Ce^{3+}, Fe^{3+}, Th^{4+} and Zr^{4+}, respectively. On the other hand, the desorption data indicated that Ce^{3+} 95 ± 5% (i.e., 65.6 ± 4 ppm) of loaded ions was only present in sodium acetate solution without contamination with Fe^{3+} or Th^{4+} or Zr^{4+}. Next, 86 ± 6% (18.1 ± 1.3 ppm) of loaded Zr^{4+} was eluted in citric acid solution, while the other metals, i.e., Fe^{3+} and Th^{4+}, were not present. Finally, 83% (i.e., ~ 54 and, 55.61 ppm) of loaded Fe and Th ions are eluted with 8 M HCl solution. Thus, Ce^{3+} (Ln^{3+}) is successfully separated out the metal ions commonly interfered with lanthanides either by batch or column techniques. By comparison between the data obtained from bath and column techniques, it can be concluded that the *S*% and *L*% values, in addition to, the amount of metal ions yield, i.e., desorbed (*D*) or eluted (*E*) were varied. This result may be due to the variations in their experimental conditions, in which there are no agitation, stirring and/or equilibrium in column technique

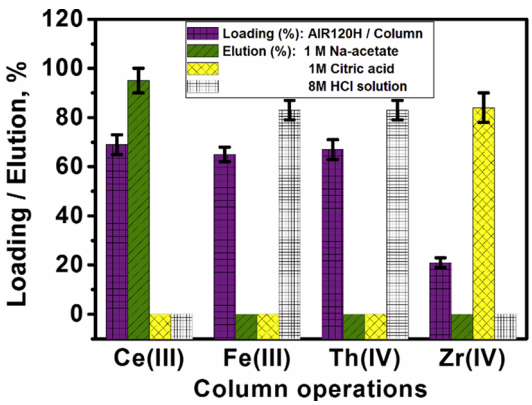

Fig. 9 Column operations of loading and elution of Ce^{3+}, Fe^{3+}, $Th^{4+}$and Zr^{4+} admixture using IR120H resin

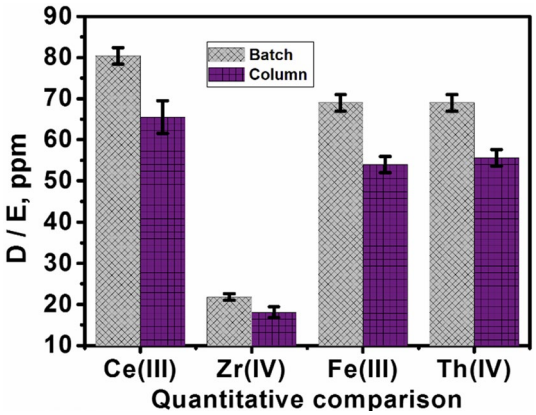

Fig. 10 Quantitative comparison for desorbed and eluted ions by batch and column techniques using IR120H resin

(Rizk et al. 2022a). The amounts of metal ions separated by batch and column techniques are reported in Fig. 10.

Table 6 The XRF measurements of high-grade monazite mineral (92%)

Element	Compound	Concentration, %
Lanthanides (35.1%)		
Ce	CeO_2	16.7
La	La_2O_3	8.8
Nd	Nd_2O_3	6.4
Pr	Pr_2O_3	1.4
Sm	Sm_2O_3	1.0
Gd	Gd_2O_3	0.8
Impurities (64.9%)		
Fe	Fe_2O_3	12.1
Zr	ZrO_2	11.6
Th	ThO_2	5.40
P	P_2O_5	10.1
Si	SiO_2	5.5
Others[a]	M-oxides	20.2

[a]Ca, Sr, Pb, Al, Mn, Ti, Zn, Cr

Table 7 The natural radioactivity levels found in monazite mineral and its chloride liquor ($LnCl_3$) (Borai et al. 2017a, b)

ID radionuclide	Monazite, Bq/kg	$LnCl_3$ liquor, Bq/L	Permitted safe limit, Bq/kg (El Afifi et al. 2019)
^{228}Ra (^{232}Th-series)	141,000 ± 2000	11,000 ± 400	< 1000
^{226}Ra (^{238}U-series)	37,000 ± 300	1900 ± 80	< 1000
^{223}Ra(^{235}U-series)	19,000 ± 400	1400 ± 30	< 1000
^{210}Pb (^{238}U-series)	2900 ± 200	2300 ± 60	< 1000
^{40}K (potassium)	< MDM[1]	< MDA	< 10,000

NR, not reported

[a]Minimum detectable activity (< 5 Bq/kg)

Application study

It is well known that monazite mineral is a complicated matrix since it contains considerable amounts of lanthanides (~ 34%) as Ln_2O_3 (e.g., Ce > La > Nd > Pr > Sm > Gd), beside high radioactivity levels of actinides (e.g., ^{232}Th and ^{235,238}U) and their respective long-lived decay progenies, e.g., radium-isotopes [(^{228}Ra, ^{226}Ra and ^{223}Ra) and radio-lead (^{210}Pb)] (Borai et al. 2017a, b). Therefore, exploration of Ln^{3+} from monazite faces opportunities such as (1) presence of the interfering metal ions such as Fe, Th, and Zr, Table 6. (2) presence an enhanced natural radioactivity above the permitted limits (IAEA 2017); Table 7. Thus, the separation of Ln^{3+} needs the next purification.

Removal of undesirable radionuclides

For this purpose, a sample of the high-grade monazite is digested by the caustic method. The produced hydroxide cake of Ln(III) is solubilized by hot concentrated HCl with stirring, then, it is filtered off to eliminate the non-reacted, suspended and/or insoluble matters. Hence, 1 mL of carrier solution containing 25 mg/mL of Ba^{2+} and Pb^{2+} is added to the lanthanide concentrate solution. Then, the lanthanides concentrate as $LnCl_3$ liquor is homogenized, adjusted to pH 2.5 ± 0.1, and left overnight. The mixture is filtered off to separate the 'insoluble residues' as a by-product away from the lanthanide concentrate as clear '$LnCl_3$ liquor.' The radiometric measurements of the products indicated that ~ 92% of natural radioactivity due to Ra^{2+}-isotopes

Table 8 The ICP-OES measurements of chloride liquor as $LnCl_3$ after deactivation

Element	Compound	Concentration, ppm
Lanthanides		
Ce	$CeCl_4$	14,410
La	$LaCl_3$	7920
Nd	$NdCl_3$	4780
Major impurities		
Fe	$FeCl_3$	ND[a]
Zr	$ZrCl_4$	ND
Th	$ThCl_4$	3110

[a]Not detected

(^{228}Ra, ^{226}Ra, $^{223}Ra^{2+}$) and radio-lead($^{210}Pb^{2+}$) is removed by co-precipitation with the carriers add and/or adsorption onto the very insoluble metal oxides or hydroxides formed at pH 2.5 ± 0.1, e.g., $Ca(OH)_2$, K_{sp} 5.5×10^{-6}; $Ba(OH)_2$, 2.6×10^{-4}, $Fe(OH)_3/Fe(OH)_{2.7}Cl_{0.3}$, 2.8×10^{-39}, $Pb(OH)_2$, 1.4×10^{-15}; $Mn(OH)_2$, 1.9×10^{-13}; $Zn(OH)_2$, 3×10^{-17} and $ZrO2(c)/ZrO(OH)_2/Zr(OH)_4$, 6.3×10^{-49} (Speight 2012; Shahr El-Din et al. 2019; El Afifi et al. 2019). As result, the activity concentration is reduced below the recommended safe limits (IAEA 2017) in the $LnCl_3$ liquor. Moreover, the ICP-OES of $LnCl_3$ liquor showed presence high concentration of Ln^{3+} and minor amount of Th^{4+} without the presence of Zr^{4+} and Fe^{3+} (not detected), Table 8. It can be said that Fe^{3+} or Zr^{4+} disappeared in $LnCl_3$ liquor due to their co-precipitation and/or adsorption onto the insoluble metal oxides or hydroxides (Borai et al. 2017a, b; El Afifi et al. 2019). Thus, the clear $LnCl_3$ liquor is ready now for the further solid phase separation by the IR120H resin using the column technique.

Separation of lanthanides from $LnCl_3$ liquor

One milliliter of the de-activated $LnCl_3$ liquor was evaporated till near dryness, then, the residue is dissolved again by 500 µL of concentrated HCl diluted by double distilled water till the pH of the solution reached pH 2 ± 0.1 (i.e., 0.01 M HCl). Assuming the previously optimized conditions assuming batch investigations, 10 mL of the diluted $LnCl_3$ mixed with 0.1 g of AIR120H resin (*V*/*m* 0.1 L/g and at room temperature) was shaken for 90 min. The mixture is filtered off. Further, the loaded AIR120H resin is equilibrated again with 1 M sodium acetate solution to desorb the loaded Ln^{3+}. Next, the solution was filtered off; the previous step was repeated with the same sample of the resin using 8 M hydrochloric acid solution for flushing the used AIR120H resin. Lanthanides and Th were selectively measured before and after equilibration of $LnCl_3$ liquor with the used resin and the solutions used for the subsequent desorption process. The concentration of the total Ln^{3+} and Th^{4+} in the prepared real sample was 92 and 14.2 ppm, respectively. After equilibration with the resin, the sorption % of total Ln^{3+} and Th^{4+} were about $82 \pm 2\%$ (~ 75.4 ppm Ln^{3+}) and

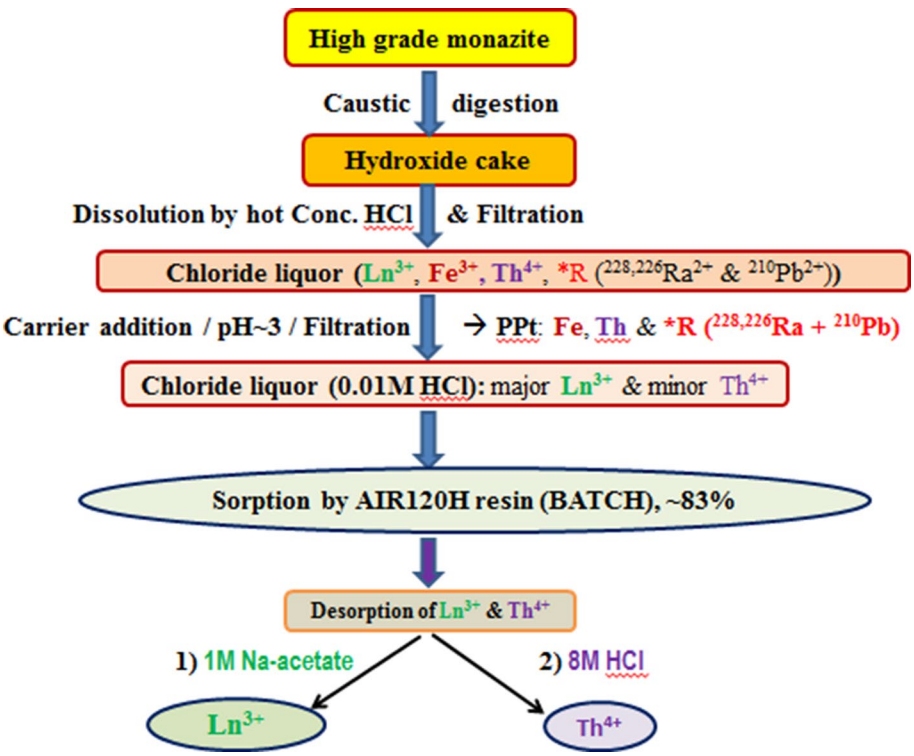

Fig. 11 A flowchart for separation and purification of lanthanides (Ln^{3+}) from monazite by Amberlite IR120H

$81 \pm 2\%$, (~ 11.5 ppm Th^{4+}), respectively. After the desorption investigations, only total Ln^{3+} are detected in sodium acetate solution without Th^{4+}. It is found that $90 \pm 5\%$ of total Ln^{3+}, i.e., ~ 68 ppm Ln^{3+}, was recovered in sodium acetate solution and $86 \pm 4\%$ of loaded Th ions was eluted after washing the AIR120H resin with 8 M HCl. Moreover, the ICP-OES measurement for sodium acetate confirmed the presence of Ce, La and Nd as major elements without interfering metal ions. Figure 11 shows the flowchart for separation and purification of lanthanides (Ln^{3+}) from monazite by Amberlite IR120H.

Conclusion

Briefly, the sorption and desorption processes in this study were verified under optimal conditions. The order of the sorption effectiveness (S, %) for several acidic media was $HCl > HNO_3 > H_2SO_4$. After 90 min of equilibration in a quaternary mixture containing Fe^{3+} and Th^{4+}, the maximum separation factor between Ce^{3+} and Zr^{4+} was ~ 13, and the sorption capacity of AIR120H resin for Ce^{3+} was 8.2 mg/g. This work used pseudo-first-order and pseudo-second-order kinetic models to explain the adsorption mechanism. The findings demonstrate that these metal ions adhered to pseudo-second-order during their adsorption processes on AIR120H resin, indicating that liquid film diffusion, intra-particle diffusion, and surface adsorption coexisted. This study was successful in isolating Ce^{3+}, an analog of lanthanides (Ln^{3+}), with 100% purity from undesirable ions such as Zr^{4+}, Fe^{3+}, and Th^{4+} using AIR120H resin as a strongly cationic exchange whether from a simulated or actual sample of the high-grade monazite. Additionally, these undesirable ions were also successfully separated from one another by desorption using different eluents such as 1 M citric acid for desorption of loaded Zr^{4+} and then the loaded Fe^{3+} and Th^{4+} ions were desorbed by 8 M HCl which also used for the flushing process of the column resin after the elution process. Therefore, after desorption of all the loaded ions and flushing the sample with 8 M HCl, the used sample of AIR120H resin can easily be reused. It is concluded that the AIR120H resin can be considered an efficient and promising cationic adsorbent to explore Ln^{3+}-concentrate in the chloride liquor ($LnCl_3$) associated with monazite processing.

Funding Open access funding provided by The Science, Technology & Innovation Funding Authority (STDF) in cooperation with The Egyptian Knowledge Bank (EKB).

Declarations

Conflict of interest The authors declared that they have no conflict of interest.

References

Abreu RD, Morais CA (2010) Purification of rare earth elements from monazite sulphuric acid leach liquor and the production of high-purity ceric oxide. Miner Eng 23:536–540. https://doi.org/10.1016/j.mineng.2010.03.010

Ali MM, El-Alfy MS, Zayed MA, Rabie KA, El-Hazek N, Aly HF (1996) Third Arab conference on the peaceful uses of atomic energy, Damascus, AAEA, pp 9–13

Ang KL, Li D, Nikoloski AN (2018) The effectiveness of ion exchange resins in separating uranium and thorium from rare earth elements in acidic aqueous sulfate media part 2 chelating resins. Miner Eng 123:8–15

Attallah MF, El Afifi EM, Shehata FA (2020) Performance of some ion exchange resins on removal of ^{241}Am(III), $^{152+154}Eu$(III), ^{99}Mo(VI), ^{137}Cs(I) and ^{60}Co(II) from simulated nuclear acidic solutions. Radiochemistry 62(5):681–688

Bhatt KD, Vyas DJ, Gupte HS, Makwana BA, Darjee SM, JianVK, (2014) Solid phase extraction, pre-concentration and sequential separation of U(VI), Th(IV), La(III) and Ce(III) by octa-*o*-methoxyresorcin[4]arene based Amberlite XAD-4 chelation resin. World J Anal Chem. 2(2):31–41

Borai EH, El Afifi EM, Shahr El-Din AM (2017a) Selective elimination of natural radionuclides during the processing of high grade monazite concentrates by caustic conversion method. Korean J Chem Eng 34(4):1099. https://doi.org/10.1007/s11814-016-0350-9

Borai EH, Hamed MM, Shahr El-Din AM (2017b) A new method for processing of low-grade monazite concentrates. J Geol Soc India 89:600–604. https://doi.org/10.1007/s12594-017-0649-0

Borai EH, Ahmed IM, Shahr El-Din AM, Abd El-Ghany MS (2018) Development of selective separation method for thorium and rare earth elements from monazite liquor. J Radioanal Nucl Chem 316(2):443–450. https://doi.org/10.1007/s10967-018-5814-4

Dakroury GA, Allan KF, Attallah MF, El Afifi EM (2020) Sorption and separation performance of certain natural radionuclides of environmental interest using silica/olive pomace nanocomposites. J Radioanal Nucl Chem 325(2):665–639. https://doi.org/10.1007/s10967-020-07237-y

Du Graedel XTE (2011) Global in-use stocks of the rare earth elements: a first estimate. Environ Sci Technol 45:4096–4101. https://doi.org/10.1021/es102836s

El Afifi EM, Attallah MF, orai EH, (2016) Utilization of natural hematite as reactive barrier for immobilization of radionuclides from radioactive liquid waste. J Environ Radioact 151:156–165. https://doi.org/10.1016/j.jenvrad.2015.10.001

El Afifi EM, Borai EH, Shahr El-Din AM (2019) New approaches for efficient removal of some radionuclides and iron from rare earth liquor of monazite processing. Int J Environ Sci Technol 16(12):7735–7746. https://doi.org/10.1007/s13762-018-02183-5

El Shahr El-Din AM, Afifi EM, Borai EH (2019) Purifcation of rare earth chloride liquor associated with high-grade monazite exploitation. J Radioanal Nucl Chem 319(3):1184. https://doi.org/10.1007/s10967-018-6389-9

Esma B, Omar A, Amine DM (2014) Comparative study on lanthanum(III) sorption onto lewatit TP 207 and l ewatit TP 260. J Radioanal Nucl Chem 299:446. https://doi.org/10.1007/s10967-013-2766-6

Eusebius LCT, Mahan A, Ghose AK, Dey AK (1977) cation exchange sorption of some metal ions from aqueous. Indian J Chem 15A:438

Fan S, Wang Y, Wang Z, Tang J, Li X (2017) Removal of methylene blue from aqueous solution by sewage sludge-derived biochar: adsorption kinetics, equilibrium, thermodynamics and mechanism. J Environ Chem Eng 5(1):601–611. https://doi.org/10.1016/j.jece.2016.12.019

Gok C, Seyhan S, Merdivan M, Yurdakoc M (2007) Separation and preconcentration of La^{3+}, Ce^{3+} and Y^{3+} using calix [4] resorcinarene impregnated on polymeric support. Microchim Acta 157:13–19. https://doi.org/10.1007/s00604-006-0646-2

Hamed MM, Hilal MA, Borai EH (2016) Chemical distribution of hazardous natural radionuclides during monazite mineral processing. J Environ Radioact 162:166–171. https://doi.org/10.1016/j.jenvrad.2016.05.028

Hamed MM, Shahr El-Din AM, Abdel-Galil EA (2019) Nanocomposite of polyaniline functionalized Tafa: synthesis, characterization, and application as a novel sorbent for selective removal of Fe(III). J Radioanal Nucl Chem 322:663–676. https://doi.org/10.1007/s10967-019-06733-0

Healy MR, Ivanov AS, Karslyan Y, Bryantsev VS, Moyer BA, Jansone-Popova S (2019) Efficient separation of light lanthanides (III) using bis-lactam phenanthroline ligands. Chem Eur J 25:6326–6331

Ho YS, Mckay G (1999) Pseudo-second order model for sorption processes. Process Biochem 34(5):451–65

IAEA (2017) IAEA safety standards for protecting people and environment. DS499, 36

Jain VK, Handa A, Sait SS, Shrivastav P, Agrawal YK (2001) Pre-concentration, separation and trace determination of lanthanum(III), cerium(III), thorium(IV) and uranium(VI) on polymer supported o-vanillinsemicarbazone. Anal Chim Acta 429:237–246. https://doi.org/10.1007/s00604-006-0646-2

Kumari A, Jha S, Patel JN, Chakravarty S, Jha MK, Pathak DD (2018) Processing of monazite leach liquor for the recovery of light rare earth metals (LREMs). Miner Eng 129:9–14. https://doi.org/10.1016/J.MINENG.2018.09.008

Lagergren S (1898) Zurtheorie der sogenennten adsorption geloster-stoffe. Kungliga Kungl Svenska Vetenskapsakad Handl 24:1–39

Marczenko Z (1976) Ellis H. Ltd., Poland

Masuda Y, Zhang Y, Yan C, Li B (1998) Studies on the extraction and separation of lanthanide ions with a synergistic extraction system combined with 1,4,10,13-tetrathia-7,16-diazacyclooctadecane and lauric acid. Talanta 46(1):203–213. https://doi.org/10.1016/s0039-9140(97)00275-0

Mayyas M, Al-Harahshehand M, Wei XY (2014) Solid phase extractive preconcentration of uranium from jordanian phosphoric acid using 2-hydroxy-4-aminotriazine-anchored activated carbon. Hydrometallurgy 149:41–49. https://doi.org/10.1016/j.hydromet.2014.07.005

Metwally SS, Rizk HE (2014) Preparation and characterization of nano-sized iron-titanium mixed oxide for removal of some lanthanides from aqueous solution. Sci Technol 49:2426–2436. https://doi.org/10.1080/01496395.2014.926457

Mokhtari M, Keshtkar AR (2016) Removal of Th(IV), Ni(II) and Fe(II) from aqueous solutions by a novel pan–tio_2 nanofiber adsorbent modified with aminopropyltriethoxy-silane. Res Chem Intermed 42:4055–4076. https://doi.org/10.1007/s11164-015-2258-0

Patawat C, Silakate K, Chuan-Udom S, Supanchaiyamat N, Andrew J, Hunt AJ, Ngernyen Y (2020) Preparation of activated carbon from *Dipterocarpus alatus* fruit and its application for methylene blue adsorption. RSC Adv 10:21082–21091. https://doi.org/10.1039/d0ra03427d

Pathania D, Sharma S, Singh P (2017) Removal of methylene blue by adsorption onto activated carbon developed from *Ficus carica* bast arab. J Chem 10:S1445–S1451. https://doi.org/10.1016/j.arabjc.2013.04.021

Rizk HE, El-Hefny NE (2020) Synthesis and characterization of magnetite nanoparticles from polyol medium for sorption and selective separation of Pd(II) from aqueous solution. J Alloys Compd 812:152041–152054

Rizk HE, Abou-Lilah RA, Elshorbagy MA, Gamal AM, Badawy NA, Ali AM (2022a) Encapsulation of ammonium molybdophosphate for removal of selected radionuclides from multicomponent solution in a fixed-bed column. Int J Environ Anal Chem. https://doi.org/10.1080/03067319.2022.2130689

Rizk HE, Shahr El-Din AM, El Afifi EM, Attallah MF (2022b) Potential separation of zirconium and some lanthanides of the nuclear and industrial interest from zircon mineral using cation exchanger resin. J Dispers Sci Technol 43(11):1642–1651. https://doi.org/10.1080/01932691.2021.1878039

Rodliyah I, Rochaniro S, Wahyudi T (2015) Extraction of rare earth metals from monazite mineral using acid method. Indones Min J 18(1):39–45

Rodríguez R, Avivar J, Leal LO, Cerdà V, Ferrer L (2016) Strategies for automating solid-phase extraction and liquid-liquid extraction in radiochemical analysis TrAC trends. Anal Chem 76:152. https://doi.org/10.1016/j.trac.2015.09.009

Rosenblum S, Fleischer M (1995) The distribution of rare-earth elements in minerals of the monazite family. Government Printing Office, Washington, p 62

Satusinprasert P, Suwanmanee U, Rattanaphra D (2015) Separation of light and middle-heavy rare earths from nitrate medium by liquid–liquid extraction. Kasetsart J Nat Sci 49(1):155–163

Shu Q, Khayambashi A, Wang X, Wei Y (2018) Studies on adsorption of rare earth elements from nitric acid solution with macroporous silica-based bis(2-ethylhexyl)phosphoric acid impregnated polymeric adsorbent. Adsorp Sci Technol 36(3–4):1065. https://doi.org/10.1177/0263617417748112

Speight JG, (2005) Lange's handbook of chemistry inorganic chemistry, 16th edn. New York: McGrawHill companies Inc. ISSN: 0748-4585, pp 155–166

Speight JG (2012) Lange's handbook of chemistry. Inorganic chemistry, solubility product constants. McGraw-Hill, New York, p 342

Talebi M, Abbasizadeh S, Keshtkar AR (2017) Evaluation of single and simultaneous thorium and uranium sorption from water systems by an electrospun PVA/SA/PEO/HZSM5 nanofiber. Process Saf Environ Prot 109:340–356. https://doi.org/10.1016/j.psep.2017.04.01

Tian M, Song N, Wang D, Quan X, Jia Q, Wuping L, Li W, Lin W (2012) Applications of the binary mixture of sec-octylphenoxyacetic acid and 8-hydroxyquinoline to the extraction of rare earth elements. Hydrometallurgy 111:109–113. https://doi.org/10.1016/j.hydromet.2011.11.002

Wang L, Yu Y, Huang X, Long Z, Cui D (2013) Toward greener comprehensive utilization of bastnaesite: simultaneous recovery of cerium, fluorine, and thorium from bastnaesite leach liquor using

HEH(EHP). Chem Eng J 215:162–167. https://doi.org/10.1016/j.cej.2012.09.126

Wang M, Zagorodny A, Muhammed M (2015) HYDRA-MEDUSA Software: hydrochemical equilibrium constant database, ignasi puigdomened inorganic chemistry. Royal Institute of Technology, Stockholm, Sweden

Wang X, Guo H, Wang F, Tan T, Wu H, Zhang H (2020) Halloysite nanotubes: an eco-friendly adsorbent for the adsorption of Th(IV)/U(VI) ions from aqueous solution. J Radioanal Nucl Chem 324:1151–1165. https://doi.org/10.1007/s10967-020-07142-4

Xu S, Zhu Q, Lin X, Lin W, Qin Y, Li Y (2021) The phase behavior of n-ethylpyridinium tetrafluoroborate and sodium-based salts ATPS and its application in 2-chlorophenol extraction. Chin J Chem Eng 33:76–82. https://doi.org/10.1016/j.cjche.2020.07.024

Zhang A, Kuraoka E, Hoshi H, Kumagai M, Chromatogr J (2004) Synthesis of two novel macroporous silica-based impregnated polymeric composites and their application in highly active liquid waste partitioning by extraction chromatography. J Chromatogr A 1061:175–182. https://doi.org/10.1016/j.chroma.2004.11.023